

Influences of porous reservoir Laplace pressure on emissions from passively fed ionic liquid electrospray sources

Daniel G. Courtney and Herbert Shea

Citation: [Applied Physics Letters](#) **107**, 103504 (2015); doi: 10.1063/1.4930231

View online: <http://dx.doi.org/10.1063/1.4930231>

View Table of Contents: <http://scitation.aip.org/content/aip/journal/apl/107/10?ver=pdfcov>

Published by the [AIP Publishing](#)

Articles you may be interested in

[Influence of ion source configuration and its operation parameters on the target sputtering and implantation process](#)

Rev. Sci. Instrum. **83**, 063304 (2012); 10.1063/1.4731009

[Proton emission from a laser ion source](#)

Rev. Sci. Instrum. **83**, 02B310 (2012); 10.1063/1.3671740

[Monoenergetic source of kilodalton ions from Taylor cones of ionic liquids](#)

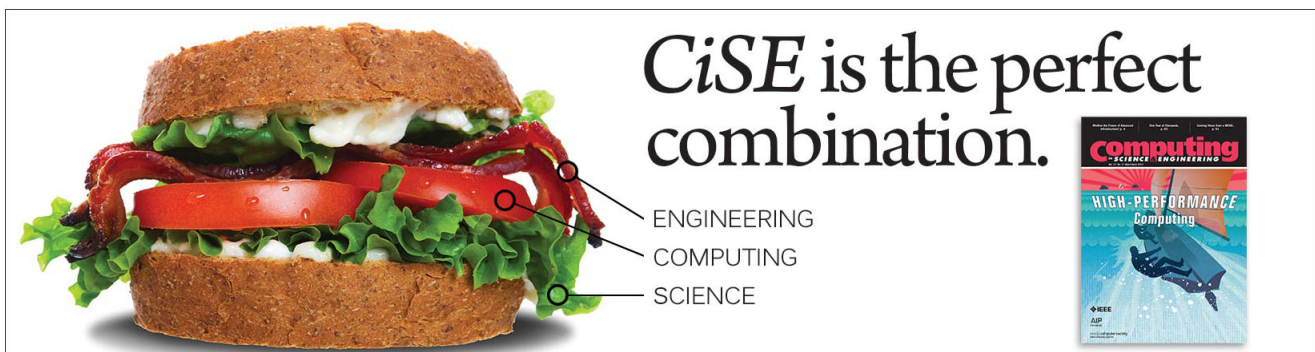
J. Appl. Phys. **101**, 084303 (2007); 10.1063/1.2717858

[Decaborane beam from ITEP Bernas ion source](#)

Rev. Sci. Instrum. **77**, 03C102 (2006); 10.1063/1.2147737

[Multiply charged ion-induced secondary electron emission from metals relevant for laser ion source beam diagnostics](#)

Rev. Sci. Instrum. **73**, 776 (2002); 10.1063/1.1431704

The advertisement features a large image of a sandwich on the left, with three callout lines pointing to different layers: 'ENGINEERING' points to the top bun, 'COMPUTING' points to the lettuce, and 'SCIENCE' points to the tomato slice. To the right of the sandwich is the text 'CiSE is the perfect combination.' in a large, serif font. Further right is a small image of a journal cover titled 'Computing in Science and Engineering' with the subtitle 'HIGH-PERFORMANCE Computing' and a blue abstract graphic.

Influences of porous reservoir Laplace pressure on emissions from passively fed ionic liquid electro spray sources

Daniel G. Courtney^{a)} and Herbert Shea

Ecole Polytechnique Federale de Lausanne (EPFL), Microsystems for Space Technologies Laboratory (LMTS), Neuchatel CH-2002, Switzerland

(Received 15 June 2015; accepted 25 August 2015; published online 8 September 2015)

Passively fed ionic liquid electro spray sources are capable of efficiently emitting a variety of ion beams with promising applications to spacecraft propulsion and as focused ion beams. Practical devices will require integrated or coupled ionic liquid reservoirs; the effects of which have not been explored in detail. Porous reservoirs are a simple, scalable solution. However, we have shown that their pore size can dramatically alter the beam composition. Emitting the ionic liquid 1-ethyl-3-methylimidazolium bis(trifluoromethylsulfonyl)amide, the same device was shown to yield either an ion or droplet dominated beam when using reservoirs of small or large pore size, respectively; with the latter having a mass flow in excess of 15 times larger than the former at negative polarity. Another source, emitting nearly purely ionic beams of 1-ethyl-3-methylimidazolium tetrafluoroborate, was similarly shown to emit a significant droplet population when coupled to reservoirs of large ($>100\ \mu\text{m}$) pores; constituting a reduction in propulsive efficiency from greater than 70% to less than 30%. Furthermore, we show that reservoir selection can alter the voltage required to obtain and sustain emission, increasing with smaller pore size. © 2015 AIP Publishing LLC.

[<http://dx.doi.org/10.1063/1.4930231>]

Ionic Liquid Ion Sources (ILIS) have recently seen significant attention as spacecraft microthrusters¹⁻⁴ and as focused ion beams.^{5,6} As thrusters, their inherently high propulsive performance metrics (power efficiency and specific impulse) rapidly deteriorate if even a small amount of droplet emission accompanies the otherwise ionic beam. Prototype arrays of ILIS have demonstrated good performance using small chip level Ionic Liquid (IL) reservoirs.^{1,2,7} However, the propellant supply must be scaled up to achieve useful mission durations. Low density porous or pooled reservoirs are therefore envisioned; yet these could significantly alter the static pressure within the IL and, as we show here, dramatically alter the droplet content and operating voltages.

ILIS are passively fed electro sprays, operated under vacuum, with a high propensity to emit at or close to a purely ionic regime (PIR).⁸ Unlike pressure or flow controlled capillary electro spray,^{9,10} passive devices establish a flow and electrical current solely controlled by the applied extraction voltage. Correspondingly, while the fluid control mechanism is routinely reported in the former, the upstream pressure of passive emitters has seen little attention.

The interfacial pressure jump across the electrified meniscus P_{int} relates to the flow rate Q , hydraulic impedance Z and reservoir pressure P_B as $P_{int} = P_B - QZ$. In vacuum, P_B due to a porous reservoir will be the static Laplace pressure, roughly $-4\gamma/D_R$, where γ is the liquid surface tension and D_R is the reservoir pore size. Hence, for porous reservoirs, or for cases where QZ is large,¹¹ P_{int} will be negative. While a negligible interfacial pressure corresponds with the familiar purely conical Taylor cone, a negative P_{int} leads to a curved

surface, flattening away from a conical tip at a length scale proportional¹² to $\gamma/|P_{int}|$.

Pantano *et al.*¹³ used numerical models to show that the applied voltage and meniscus volume consistent with Taylor cones at negative P_{int} increase and decrease, respectively. More recently, Higuera's model of the current from ILIS of fixed volume¹⁴ found that lower volumes were more stable in supporting stable ion evaporation.

We therefore ask, do conditions which can enforce a large negative P_{int} , like porous reservoirs, significantly influence ion emission stability in ILIS?

Geometries of passively fed electro spray in the PIR have expanded beyond externally wet roughened surfaces^{7,15} to include microfabricated capillaries³ and porous structures.^{1,2,16} Here, we have used porous sources, schematized in Figure 1. To control the maximum level of P_{int} , we have interchanged the porous reservoir coupled to an unchanged emitter substrate. Reservoirs of differing pore diameter, and therefore Laplace pressure were used to control the negative back pressure feeding the emitter. The pore diameters of all reservoirs were at least $10\times$ larger than those of the emitting substrate; ensuring changes to the total hydraulic impedance were negligible.

Two emission sources were cut from porous borosilicate glass using a Computer Numerical Control (CNC) milling process described previously.⁴ One was operated with the IL 1-ethyl-3-methylimidazolium tetrafluoroborate (EMI-BF₄) and the other with 1-ethyl-3-methylimidazolium bis(trifluoromethylsulfonyl)amide (EMI-Im). One 7 mm long triangular prism was machined per 10 mm diameter, 3 mm thick disc of Duran Group P5 grade material (1.0–1.6 μm pores), Figure 2. The sharp (10's of μm curvature) edge achieved with this simple, microfabrication-free, approach supports multiple emission sites summing to 10's of μA of highly

^{a)}dcourtney@alum.mit.edu

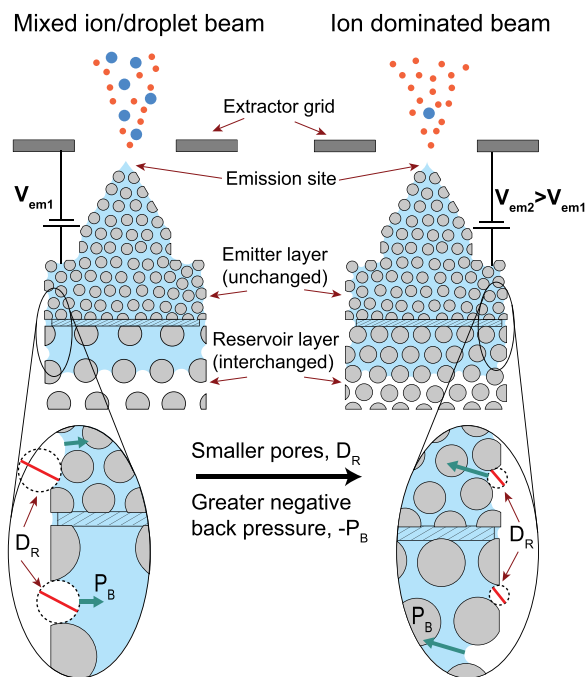


FIG. 1. A porous electro spray source has been matted with reservoirs of differing pore size. The beam composition and current-voltage characteristics are found to be strongly dependent on the accompanying change in negative back pressure.

ionic emission.⁴ This emission was controlled by an electric potential applied between the IL and a 350 μm wide, 100 μm thick molybdenum extractor grid, which was vertically aligned to within $\pm 30 \mu\text{m}$ of the apex.

Additional Duran Group 10 mm diameter porous borosilicate discs have been used as reservoirs. First bubble point pressure measurements¹⁷ for each reservoir/IL combination were used to approximately quantify their negative Laplace pressures and thereby $-P_B$ for the system. That is, larger bubble points indicate smaller pores and a stronger negative back pressure. Five porosity grades were used: P4 ($D_R \approx 10\text{--}16 \mu\text{m}$), P3 ($D_R \approx 16\text{--}40 \mu\text{m}$), P2 ($D_R \approx 40\text{--}100 \mu\text{m}$), P1 ($D_R \approx 100\text{--}160 \mu\text{m}$), and P0 ($D_R \approx 160\text{--}250 \mu\text{m}$). Measured bubble points ranged from roughly 0.9 kPa to 8.7 kPa for the P0 through P4 grades, respectively.

The reservoirs were hydraulically coupled to the emitter substrate via a layer of filter paper (Whatman Qualitative No. 1) which, along with the emitting substrate, was constantly saturated with IL. Prior to each test, the devices were reassembled and 30–40 μl of IL was added to these saturated layers, ensuring IL was drawn into the new reservoir until reaching equilibrium. To aid in demonstrating that the

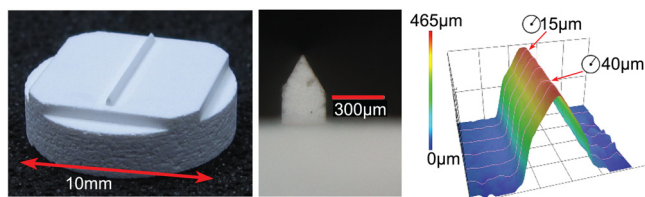


FIG. 2. Images of the emitter structures. A small CNC mill was used⁴ to form a prominent triangular prism with a sharp apex ($\sim 15 \mu\text{m}$ to $40 \mu\text{m}$ radius of curvature) on the surface of a 10 mm diameter porous borosilicate filter disc.

reported results were due to reservoir selection, and not other spurious influences, reservoirs were not tested sequentially by pore size.

Beam compositions via Time of Flight (ToF) spectrometry have been recorded for each IL/reservoir combination using the apparatus described in Ref. 4. Unlike in the reference, the emission potential was alternated at 2 Hz at all times, including during ToF measurements. Alternation,¹⁸ and an inherent distal contact to the IL¹⁹ were employed to suppress electrochemical reactions. The ToF gate signal, a 2 Hz symmetric square wave, was synchronized to activate 130 ms after alternating to the polarity of interest; preventing charged particles from entering the flight tube once active. Each ToF trace indicates the current subsequently collected by a Faraday-type detector. Flight times t have been converted²⁰ to a mass to charge-number ratio (m/z), without assuming a charge state z , using Equation (1); where L and V_{em} are the flight tube length and emitter voltage, respectively. This conversion disambiguates measurements made at difference voltages and permits ready identification of the singly charged ($z=1$) ion species emitted from the IL. Presented traces were averaged over 45 consecutive oscilloscope recordings and are normalized by the detected current just prior to gating

$$\frac{m}{z} = \frac{t^2}{L^2} 2e|V_{em}|. \quad (1)$$

Differing interfacial pressures were anticipated to alter operating voltages for each device. Hence, instead of at a consistent voltage, ToF data were taken at beam currents within 20% of 20 μA . A level achieved in all tests and well beyond the minimum starting voltage.

When emitting negative species from EMI- BF_4 , a distinct population of high m/z species was recorded whenever reservoirs of weak negative back pressure (P0 and P1) were installed, see Figure 3. This tail extended up to species with 10's of kDa m/z ; consistent with a population of small droplets (e.g., Ref. 21). When using P3 reservoirs of relatively small pore size, a nearly purely ionic (in terms of current) emission was achieved. Referring to the indicated test order, the droplet tail was removed, reinstated then removed again through selection of the reservoir. Measurements at positive polarity were relatively droplet free; however, a small

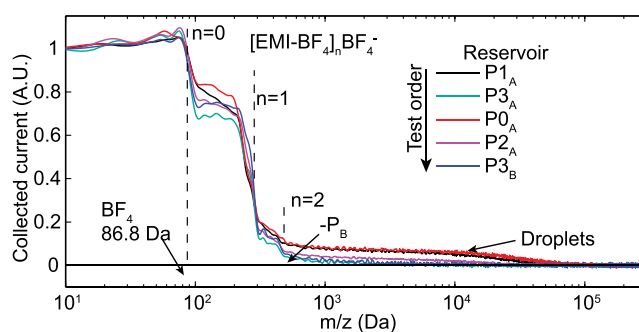


FIG. 3. ToF traces of negative EMI- BF_4 emission indicating the emergence of a small droplet current within a largely ionic beam when coupling the same device to reservoirs of relatively weak negative Laplace pressure (lower P grade). Subscripts A and B distinguish repetitions using the same P grade.

population of high m/z species was again removed when using P3 grade reservoirs, these traces are available in supplemental Fig. S1 at Ref. 22.

Changes in droplet content were more evident when emitting EMI-Im, Figure 4. Using P1 reservoirs with relatively large pores, droplets and highly solvated cluster-ions accounted for nearly half of the beam current at negative polarity. Again alternating back and forth between reservoirs, this population and its maximum mass were consistently decreased when moving to reservoirs with smaller pores and thereby stronger negative back pressure; eventually reaching an ion dominated state when a P4 reservoir was installed. Of note, the positive EMI⁺, emission mode again showed a reduced propensity for droplet emission compared with the negative state, regardless of the reservoir.

The trend towards an increasingly ionic beam when enforcing a stronger negative back pressure is further summarized in Figure 5. Here current fractions, with respect to the pre-gate signal, are indicated for each species when emitting EMI-Im. Due to the lack of discernible steps for highly solvated cluster ions we broadly refer to all current due to species with m/z greater than trimer ions and extending to many kDa as droplets. These large m/z particles constituted $\sim 50\%$ of the beam at negative polarity with P1 reservoirs (~ 1.2 kPa bubble point), yet less than 10% with the P4 grade (~ 8.7 kPa bubble point). The current fractions due to monomer ($n=0$), dimer ($n=1$), and trimer ($n=2$) species are also indicated. At both polarities dimers dominated the ion contribution although the monomer fraction increased with increasing reservoir bubble point (stronger negative back pressure).

Despite consistent operation near $20 \mu\text{A}$ of emission, heavy drops within the beam are indicative of very large

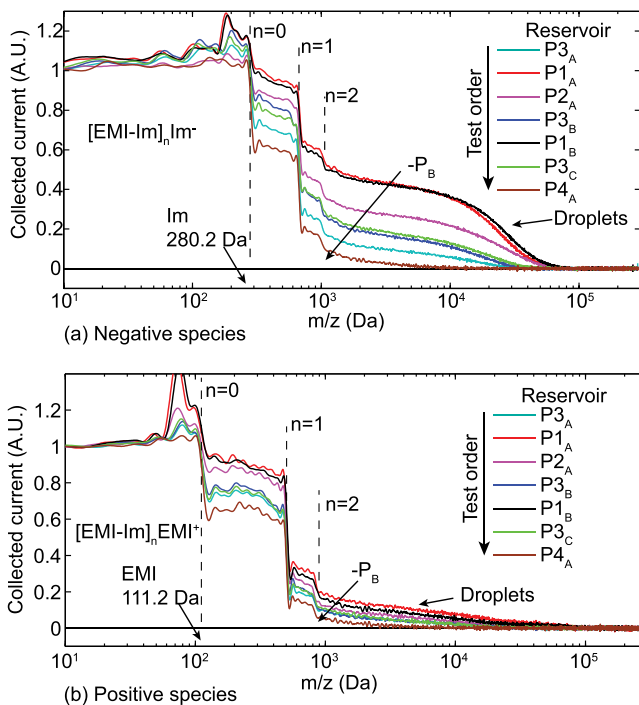


FIG. 4. ToF traces of EMI-Im emission demonstrating the suppression of droplet mass and current achieved by coupling the source to porous reservoirs of large negative Laplace pressure (higher P grade). Subscripts A, B, and C distinguish repetitions using the same reservoir P grade.

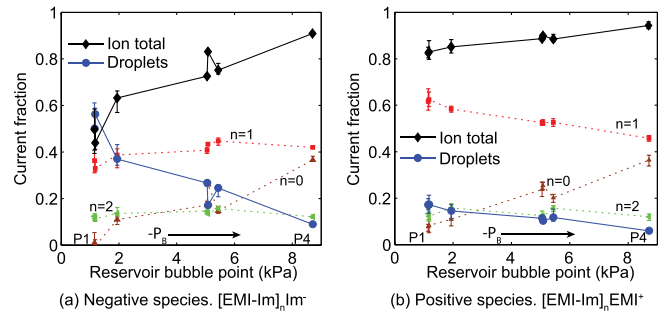


FIG. 5. The fraction of current due to ions (trimer and smaller) increased relative to droplets (larger species) with increasing reservoir bubble point (larger negative Laplace pressure). Constituent monomer ($n=0$), dimer ($n=1$), trimer ($n=2$) ion current fractions are also indicated.

changes in the mass flow rate between tests. Mass flow rates were calculated via integration of the ToF curves using Equation (2), as in Ref. 20. The integral has been separated into ion (flight times up to those for trimer ions) and droplet (larger m/z) contributions. Noting that the latter also includes some contribution, indistinguishable in the ToF data, due to highly solvated cluster ions. $F(t)$ is a small correction factor accounting for ion fragmentation during acceleration.²³ Non-dimensional flow rates ϕ_{ion} and ϕ_{drop} , due to ions and droplets, respectively, were determined via a scaling by $m_{EMI} I/e$, the mass flow that would result if all species were singly charged and with mass $m_{EMI} = 111.2$ Da. These parameters⁴ isolate changes in mass flow due to beam composition from those due to variances in the recorded current

$$\dot{m} = -\frac{2V_0}{L^2} \left[\int_0^{t_{n=2}} t^2 F(t) I dt + \int_{t_{n=2}}^{\infty} t^2 F(t) I dt \right], \quad (2)$$

$$\dot{m} = \frac{m_{EMI}}{e} I [\phi_{ion} + \phi_{drop}]. \quad (3)$$

When emitting EMI-BF₄ using the P0 and P1 reservoirs with bubble point pressures less than 1.4 kPa, the mass flow rate contribution due to droplets and was at least double that due to ions for both polarities, Figure 6(a). However, using P3 reservoirs with bubble points in excess of 7 kPa, the total mass flow rate was reduced by roughly 2 and 6 times for positive and negative emissions, respectively, with droplets contributing less than 40% to the total. The same behaviour was

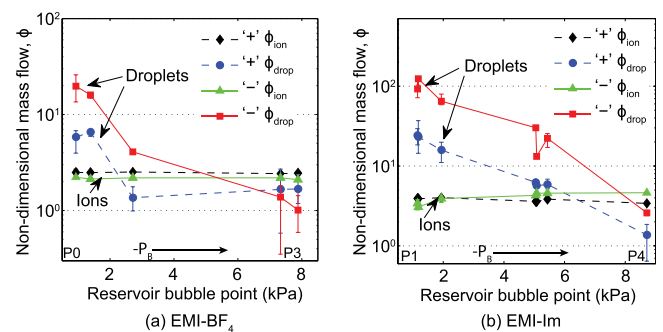


FIG. 6. Non-dimensional mass flow rates, by Equation (3), indicate droplets dominated the mass flow with reservoirs of weak Laplace pressure yet contributed less than ions using reservoirs with stronger Laplace pressure. Error bars indicate min./max. values over 2–6 repeated ToF measurements.

more pronounced using the EMI-Im emission source, Figure 6(b). Here the total, droplet dominated, mass flow rate was reduced by more than an order of magnitude when using reservoirs which enforced stronger negative back pressure; eventually becoming ion dominated. In particular, using the P1 reservoirs over 97% of the negative polarity mass flow was due to droplets. However, after coupling the same device to a P4 grade reservoir with a bubble point of roughly 8.7 kPa, the total mass flow rate was 15 times smaller and droplets contributed only about 35% to the total.

Spurious ToF signals rising well above 1 in Fig. 4 are consistent with populations of low speed monomers, likely disassociated from relatively slow droplets or clusters, located within the gate assembly when triggered, then accelerated through the gate voltage (± 3000 V). These features had a negligible impact on the reported mass flow rate calculations using Equation (2).

Current-voltage (IV) characteristics were also measured with each device. Referring to Figure 7, similar beam currents from EMI-BF₄ required increasingly larger voltages when reservoirs with smaller pores, and thereby stronger negative back pressure, were installed. Specifically, beam currents near $-20 \mu\text{A}$, where the ToF measurements in Fig. 3 were obtained, required approximately -1750 V using the relatively weak P0 grade reservoir yet between -2200 V and -2400 V for the two experiments using P3 grade reservoirs; although the latter did not yield identical IV curves. Higher voltages are consistent with increasingly larger negative interfacial pressures, P_{int} . Therefore, considering the higher mass flow rates observed with weaker reservoirs, these IV curve transitions indicate that the negative back pressures obtained via the selected reservoirs were much greater than the pressure drops due to flow impedance. Similar, although less pronounced, IV trends were observed when emitting EMI-Im. There $\pm 20 \mu\text{A}$ beam currents were recorded between $+1650/-1750$ V and $+1900/-2050$ V for the P1 and P4 grade reservoirs, respectively see supplemental Fig. S2 at Ref. 22 for these IV data. The significantly higher mass flow rates with weak reservoirs in that case could have led to a reduction in the degree to which the reservoir was an independent control of interfacial pressure.

A previous study⁴ using similar devices operated in an ion dominated configuration, showed no discernable trend in beam composition versus emitter voltage, and such parameterization was not performed here. However, with conditions

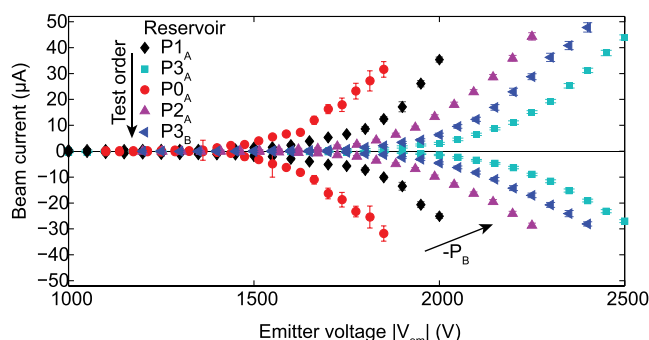


FIG. 7. Emitting EMI-BF₄, higher potentials were required for reservoirs with smaller pores and thereby stronger negative back pressures. Error bars indicate standard deviations over 3 s of data.

for droplet emission now identified, further study of voltage effects in that regime is warranted.

In the context of spacecraft propulsion, the beam composition transitions observed with each source represent significant inconsistencies in the corresponding specific impulse I_{sp} (thrust per unit mass flow rate) and propulsive power efficiency η_{prop} . (beam power per input electrical power). Using the standard ToF based expressions outlined in Ref. 20, the I_{sp} was about 2300 s and η_{prop} . about 76% at positive polarity when emitting EMI-Im using the P4 grade reservoir. However, when using P1 reservoirs with relatively large pores these metrics fell to roughly 700 s and 45%, respectively. Similarly, compared with the ion dominated EMI-BF₄ beam obtained using P3 grade reservoirs, the seemingly small by current population of droplets induced by using P0 or P1 grade reservoirs decreased η_{prop} . from over 70% to less than 30% and I_{sp} from over 3000 s to less than 650 s. Therefore, although potentially low in mass, integration of loosely packed or open reservoir geometries must be carefully considered or performance may be jeopardized.

These observations also provide information pertinent to theoretically understanding emissions from ILIS. Specifically, existing modelling approaches such as electrohydro-dynamic models of the interface²⁴ or molecular dynamics simulations²⁵ typically either do not consider a significant static pressure jump at the interface or assume a positive back pressure. While not necessarily a significant force near the emission site apex; our results indicate that negative internal pressures could be an important contributor to ensuring stability of an ion emitting meniscus. Which, at the -7 to -8 kPa maximum interfacial pressures enforced when near the PIR here, will have flattened on the μm scale. Furthermore, the differing behaviours between EMI⁺ and anion emissions are noteworthy in that they indicate a species dependence in addition to or beyond IL bulk property dependencies.

In conclusion, even when employing a passive feeding approach, the upstream pressure of an ILIS is important and can alter both the ion/droplet content and operating voltage. The presented data indicate that further experimental and theoretical investigations should include particular attention to the case, likely prevalent in ILIS, where interfacial Laplace pressures are large and negative.

This work has been supported in part through ESA NPI Contract No. 4000109063/13/NL/PA.

¹D. G. Courtney, H. Q. Li, and P. Lozano, *J. Phys. D: Appl. Phys.* **45**, 485203 (2012).

²C. Coffman, L. Perna, H. Li, and P. C. Lozano, in *49th AIAA Joint Propulsion Conference and Exhibit* (San Jose, CA, 2013).

³S. Dandavino, C. Ataman, C. N. Ryan, S. Chakraborty, D. G. Courtney, J. P. W. Stark, and H. Shea, *J. Micromech. Microeng.* **24**, 075011 (2014).

⁴D. G. Courtney, S. Dandavino, and H. Shea, "Comparing Direct and Indirect Thrust Measurements from Passively Fed and Highly Ionic Electrospray Thrusters," *J. Propul. Power* (in press).

⁵T. P. Fedkiw and P. C. Lozano, *J. Vac. Sci. Technol.*, **B 27**, 2648 (2009).

⁶C. Perez-Martinez, S. Guilet, N. Gogneau, P. Jegou, J. Gierak, and P. Lozano, *J. Vac. Sci. Technol.*, **B 28**, L25 (2010).

⁷F. A. Hill, P. P. D. Leon, and L. F. Velázquez-García, in *17th International Conference on Solid-State Sensors, Actuators and Microsystems, Transducers* (IEEE, 2013), pp. 2644–2647.

- ⁸P. Lozano and M. Martínez-Sánchez, *J. Colloid Interface Sci.* **282**, 415 (2005).
- ⁹I. Romero-Sanz, R. Bocanegra, M. Gamero-Castano, J. F. de la Mora, and P. Lozano, *J. Appl. Phys.* **94**, 3599 (2003).
- ¹⁰G. Lenguito and A. Gomez, *J. Microelectromech. Syst.* **23**, 689 (2014).
- ¹¹R. Krpoun, K. L. Smith, J. P. W. Stark, and H. Shea, *Appl. Phys. Lett.* **94**, 163502 (2009).
- ¹²J. F. de la Mora, *Annu. Rev. Fluid Mech.* **39**, 217 (2007).
- ¹³C. Pantano, A. M. Ganan-Calvo, and A. Barrero, *J. Aerosol Sci.* **25**, 1065 (1994).
- ¹⁴F. J. Higuera, *Phys. Rev. E* **77**, 026308 (2008).
- ¹⁵B. Gassend, L. F. Velasquez-Garcia, A. I. Akinwande, and M. Martinez-Sanchez, *J. Microelectromech. Syst.* **18**, 679 (2009).
- ¹⁶R. S. Legge and P. C. Lozano, *J. Propul. Power* **27**, 485 (2011).
- ¹⁷ASTM-F316-03, Standard test methods for pore size characteristics of membrane filters by bubble point and mean flow pore test, <http://www.astm.org/Standards/F316.htm>, 2011).
- ¹⁸P. Lozano and M. Martínez-Sánchez, *J. Colloid Interface Sci.* **280**, 149 (2004).
- ¹⁹N. Brikner and P. C. Lozano, *Appl. Phys. Lett.* **101**, 193504 (2012).
- ²⁰M. Gamero-Castano and V. Hruby, *J. Propul. Power* **17**, 977 (2001).
- ²¹R. Alonso-Matilla, J. Fernández-García, H. Congdon, and J. F. de la Mora, *J. Appl. Phys.* **116**, 224504 (2014).
- ²²See supplementary material at <http://dx.doi.org/10.1063/1.4930231> for EMI-BF₄ positive ToF traces and EMI-Im IV data.
- ²³D. G. Courtney and H. Shea, *J. Prop. Power* **31**(5), 1500 (2015).
- ²⁴F. J. Higuera, *Phys. Rev. E* **69**, 066301 (2004).
- ²⁵A. Borner, P. Wang, and D. A. Levin, *Phys. Rev. E* **90**, 063303 (2014).